

# Global Biogeochemical Cycles

## RESEARCH ARTICLE

10.1029/2019GB006202

### Key Points:

- COS emissions increased after UV exposure of soil samples from three European soils
- Primary abiotic driver of COS cycling differs between three European soils

### Supporting Information:

- Supporting Information S1

### Correspondence to:

F. Kitz,  
florian.kitz@uibk.ac.at

### Citation:










Kitz, F., Spielmann, F. M., Hammerle, A., Kolle, O., Migliavacca, M., Moreno, G., et al. (2020). Soil COS exchange: A comparison of three European ecosystems. *Global Biogeochemical Cycles*, 34, e2019GB006202. <https://doi.org/10.1029/2019GB006202>

Received 27 FEB 2019

Accepted 18 FEB 2020

Accepted article online 22 FEB 2020

## Soil COS Exchange: A Comparison of Three European Ecosystems

Florian Kitz<sup>1</sup> , Felix M. Spielmann<sup>1</sup> , Albin Hammerle<sup>1</sup> , Olaf Kolle<sup>2</sup> , Mirco Migliavacca<sup>2</sup> , Gerardo Moreno<sup>3</sup> , Andreas Ibrom<sup>4</sup> , Dmitrii Krasnov<sup>5</sup>, Steffen M. Noe<sup>5</sup> , and Georg Wohlfahrt<sup>1</sup> 

<sup>1</sup>Institute of Ecology, University of Innsbruck, Innsbruck, Austria, <sup>2</sup>Max Planck Institute for Biogeochemistry, Jena, Germany, <sup>3</sup>Forest Research Group, Universidad de Extremadura, Plasencia, Spain, <sup>4</sup>Department of Environmental Engineering, Technical University of Denmark, Kongens Lyngby, Denmark, <sup>5</sup>Institute of Agricultural and Environmental Sciences, Estonian University of Life Sciences, Tartu, Estonia

**Abstract** The potential of carbonyl sulfide (COS) flux measurements as an additional constraint for estimating the gross primary production depends, among other preconditions, on our understanding of the soil COS exchange and its contribution to the overall net ecosystem COS flux. We conducted soil chamber measurements of COS, with transparent chambers, in three different ecosystems across Europe. The in situ measurements were followed by laboratory measurements of soil samples collected at the study sites. The soil samples were exposed to UV radiation to investigate the role of photo-degradation for COS exchange. In situ and laboratory measurements revealed pronounced intersite and intrasite variability of COS exchange. In situ COS fluxes were primarily governed by radiation in the savannah-like grassland (SAV), soil temperature and intrasite heterogeneity in the deciduous broadleaf forest, and soil water content and intrasite heterogeneity in the evergreen needleleaf forest. The soil of the ecosystem with the highest light intensity incident on the soil surface, SAV, was a net source for COS, while the soils of the other two ecosystems were COS sinks. UV radiation increased COS emissions and/or reduced COS uptake from all soil samples under laboratory conditions. The impact of UV on the COS flux differed between soil samples, with a tendency toward a stronger response of the COS flux to UV radiation exposure in samples with higher soil organic matter content. Our results emphasize the importance of photo-degradation for the soil COS flux and stress the substantial spatial variability of soil COS exchange in ecosystems.

## 1. Introduction

Measurements of the trace gas carbonyl sulfide (COS) have been discussed as a promising tool for inferring gross primary production (GPP) and stomatal conductance at the ecosystem scale (Sandoval-Soto et al., 2005; Seibt et al., 2010; Wehr et al., 2017; Whelan et al., 2018; Wohlfahrt et al., 2012). COS sparked the interest of researchers because its uptake by plants is closely linked to the uptake of CO<sub>2</sub> (Seibt et al., 2010). Both gases enter the leaf via similar pathways and are subsequently consumed by the same enzymes, especially the enzyme carbonic anhydrase (CA) (Seibt et al., 2010; Stimler et al., 2010). So far, no COS emissions from vascular plants have been reported. This would in theory and in the absence of other ecosystem sources and sinks equate the measured COS flux at the ecosystem level to the COS uptake by plants, which could be used to infer the CO<sub>2</sub> plant uptake. COS and CO<sub>2</sub> measurements together, both on the ecosystem level, could therefore improve the partitioning of the net ecosystem CO<sub>2</sub> flux into GPP and respiration.

If COS uptake is indeed primarily driven by plant uptake, it might be a useful GPP proxy. Other sinks and sources of COS, apart from plants, should then either be negligible or easy to parameterize. Soil is potentially the largest nonleaf contributor to ecosystem COS uptake because it contains a multitude of organisms equipped with CA (Conrad, 1996; Meredith et al., 2019; Ogawa et al., 2016; Seibt et al., 2006; Wingate et al., 2008). In addition to CA, other enzymes were found to hydrolyze COS, among them RuBisCO (Lorimer & Pierce, 1989), nitrogenase (Seefeldt et al., 1995), CO dehydrogenase (Ensign, 1995), and CS<sub>2</sub> hydrolase (Smeulders et al., 2013). Substantial COS consumption by CA in soils has been shown by laboratory experiments (Kesselmeier et al., 1999; Meredith et al., 2019). Together with in situ measurements of soil COS fluxes (Steinbacher et al., 2004; Yi et al., 2007), these findings underline the role of soil as a substantial COS sink. Attempts to close the COS budget on the global scale characterized oxic soils as COS sinks (Berry

©2020. The Authors.

This is an open access article under the terms of the Creative Commons Attribution License, which permits use, distribution and reproduction in any medium, provided the original work is properly cited.

et al., 2013; Kettle et al., 2002; Launois et al., 2015; Montzka et al., 2007). Recent mechanistic soil COS flux models (Ogée et al., 2015; Sun et al., 2015) led to similar results, consolidating the role of oxic soils as a net COS sink. But there is also evidence for oxic soils acting, under hot, dry, and/or high-light conditions, as a net source for COS (Florian Kitz et al., 2017; Maseyk et al., 2014; Meredith et al., 2018; Whelan & Rhew, 2015), presumably driven by abiotic production of COS from precursors of biotic origin (Meredith et al., 2018). The motivation to understand how soil COS fluxes vary with soil moisture, soil temperature, and radiation is therefore growing, since more knowledge is needed to adequately represent the soil COS exchange in models (Whelan et al., 2018). Advances have been made in understanding the impact of soil moisture on the soil COS flux by recent laboratory studies (Bunk et al., 2017; Kaisermann, Jones, et al., 2018), which investigated soil samples from different ecosystems, concluding that COS production increases under drier conditions. Bunk et al. (2017) showed that soil samples can act as both a net COS sink and source depending on their soil moisture. Knowledge about the light contribution to COS emissions from soil is much scarcer, with only few studies (Meredith et al., 2018; Whelan & Rhew, 2015) investigating the effect of radiation under controlled conditions in the laboratory. Data for in situ measurements examining the link between radiation and soil COS exchange is equally scarce (Florian Kitz et al., 2017), since most studies used opaque chambers (Berkelhammer et al., 2014; Maseyk et al., 2014; Sun et al., 2016), therefore excluding any radiation effect on decomposition (Yanni et al., 2015). From studies investigating the ocean (von Hobe, 2003), a lake (Du et al., 2017), and precipitation (Mu et al., 2004) we know that especially the energy-rich UV fraction of the solar spectrum is involved in COS production. COS production in seawater was the highest at shorter wavelengths and decreased with increasing wavelengths (in an investigated range of 280–380 nm) (Zepp & Andreae, 1994).

The magnitude and sign of soil COS fluxes varies between ecosystems (Liu et al., 2010; Maseyk et al., 2014; Yi et al., 2007), and if our goal is a robust global estimate of the soil COS flux, we need more data from different soils. But processes in soils, for example, respiration, can vary greatly within ecosystems (Li et al., 2017; Wang et al., 2006) depending on the heterogeneity of the system, which should incentivize scientists to also cover the intrasite heterogeneity of soil COS fluxes.

We investigated three different ecosystems across Europe to address shortcomings in our current knowledge on soil COS fluxes (Whelan et al., 2018), especially the importance of abiotic versus biotic controls and the magnitude of small-scale heterogeneity. We conducted in situ measurements in an oak savannah-like grassland (SAV) in Spain, a deciduous broadleaf forest (DBF) in Denmark, and an evergreen needleleaf forest (ENF) in Estonia with transparent soil chambers. The in situ setup allowed us to address the following hypotheses: soil COS fluxes (I) are primarily driven by differences in radiation; (II) vary in response to other abiotic and biotic site characteristics such as different light, temperature, and soil moisture conditions; and (III) can change with small-scale variations in abiotic and biotic conditions within a site. Soil samples were collected from the investigated sites in addition to the in situ measurements and were compared to each other in the dark and under UV-A exposure under controlled conditions in the laboratory. This approach allowed for “real-world” data, that is, from an intact soil column and the full set of environmental parameters, to be combined with data derived from a controlled system, that is, the laboratory.

## 2. Material and Methods

### 2.1. Sites

#### 2.1.1. Savannah-Like Grassland

The FLUXNET site (Site-ID: ES-LMa) Las Majadas del Tietar (39°56′29.4″N, 5°46′24.1″W) is located in the province of Cáceres in Spain at an altitude of 260 m above sea level. The climate is Mediterranean with a mean annual temperature of 16 °C and annual rainfall of 700 mm (Perez-Priego et al., 2017). The vegetation is described as a holm oak savannah-like grassland, grazed by cows, with tree canopy coverage of about 20%. The dominant tree species is *Quercus ilex*, the grass layer is dominated by *Vulpia bromoides*, *Vulpia geniculata*, *Trifolium subterraneum*, and *Ornithopus compressus*. The soil was classified as Abrupt Luvisol (IUSS Working Group WRB, 2006). For more details about the study site, see Lopez-Sangil et al. (2011) and Weiner et al. (2018).

#### 2.1.2. Deciduous Broadleaf Forest

The FLUXNET site (Site-ID: DK-Sor) Sorø (55°29′9.24″N, 11°38′40.56″E) is located on the Danish Island of Zealand at an altitude of 40 m above sea level. The climate is temperate maritime with a mean annual

temperature of 8.5 °C and mean annual precipitation of 564 mm. The site is located in a DBF dominated by European beech (*Fagus sylvatica*). The forest is managed with an average thinning of 2% per year. The soil was classified as either Alfisols or Mollisols with a 10–40 cm deep organic layer. For more details about the study site, see Pilegaard et al. (2011) and Wu et al. (2013).

### 2.1.3. Evergreen Needleleaf Forest

The SMEAR site Järvselja (58°16'39.416"N, 27°18'29.637"E) is located in southeastern Estonia near Lake Peipsi. The climate is temperate with a mean annual temperature of 4–6 °C and annual precipitation of 500–750 mm. The site is located in a hemiboreal forest dominated by Norway spruce (*Picea abies*). The ground vegetation consists of *Oxalis acetosella*, *Vaccinium myrtillus*, *Calamagrostis arundinacea*, *Convallaria majalis*, *Melampyrum pratense*, and several moss species (at especially moist location even *Sphagnum* spp.). The soil was classified as Haplic Gleysol (eutric) with a thick humus horizon. The forest floor has a distinct structure, with elevations, which consist of decomposing tree stubs and litter, and depressions, lower, typically very wet, areas. For more details about the study site, see Noe et al. (2011, 2015).

## 2.2. In Situ Measurements

In situ measurements were done in May (SAV), June (DBF), and August (ENF) of 2016. At each site, 6–9 stainless steel (SAE grade: 316 L) rings were inserted 5 cm into the soil and remained in place for the whole month. The aboveground vegetation, if any, was removed. Some small patches of moss remained inside the ring at ENF, because removing these was not possible without a severe disturbance of the top surface layer. Litter was not removed from the soil surface in the chambers, since its contribution to the COS flux was found to be significant (Sun et al., 2016) and is often inseparable from the soil under natural conditions. Since litter (in the DBF and ENF) and a little bit of moss (in the ENF) was inside the rings, the term soil includes moss and litter typical for each site with regard to the in situ measurements to avoid introducing a new term. We attempted to cover the heterogeneity of the ecosystems by placing rings in different locations, which had distinct features as explained below. In SAV rings were placed under a tree (T), in the open grassland (O), and in between (I). In the DBF measurements were performed with chambers containing litter and chambers without litter, but only the chambers with litter were used in the analyses (to see how the rings with litter compare to the rings without litter, see supporting information Figure 1). In DBF rings were placed in areas with low (LV), medium (MV), and high (HV) surrounding ground vegetation. In ENF rings were placed on top of elevations (E) and in depressions (D) forming the characteristic microrelief of the forest floor at the site.

COS and CO<sub>2</sub> concentrations were measured with a Quantum Cascade Laser (QCL) Mini Monitor (Aerodyne Research, Billerica, MA, USA) at a wave number of ca. 2056 cm<sup>-1</sup>. The QCL was operated at a pressure of 20 Torr using a built-in pressure controller and temperature of the optical bench and housing controlled to 35 °C. Fitting of absorption spectra at 1 Hz, storing of calculated mole fractions, and switching of zero/calibration valves, control of pressure lock, and other system controls were done by the TDLWintel software (Aerodyne Research, Billerica, MA, USA). The QCL was housed in a temperature-regulated custom-built case (DE Casebuilder.com GmbH, Hamburg, Germany). A handheld sensor (WET-2, Delta-T Devices, Cambridge, England) was used to measure soil water content (SWC) and soil temperature at a soil depth of 5 cm next to the rings simultaneously with the soil chamber measurements. Photosynthetic photon flux density (PPFD) was measured with a line quantum sensor (SQ-316-SS, Apogee, USA). Environmental parameters measured during the campaigns are summarized in Figure 1.

To measure the soil flux a fused silica bell, transmitting light between 170 and 5,000 nm was placed in a water-filled channel on top of a stainless steel ring (see supporting information for a sketch of the experimental setup, Figure S2). All tubing and fittings used were either made of perfluoroalkoxy alkane (PFA) or stainless steel. Each measurement cycle started with air being drawn with approximately 1.5 L/min from a tube outside, but near the chamber to quantify the ambient concentration, while the chamber line was flushed at the same flow rate. After 5 min, the lines were switched and the air in the headspace of the chamber was measured until a steady state was reached (11.6 ± 4.6 min); meanwhile, the ambient line was flushed at the same flow rate. Afterwards, the ambient concentration was measured a second time and a linear interpolation was performed to estimate the ambient concentration at the time of the steady state conditions within the chamber. The soil COS and CO<sub>2</sub> flux was calculated according to equation (1).

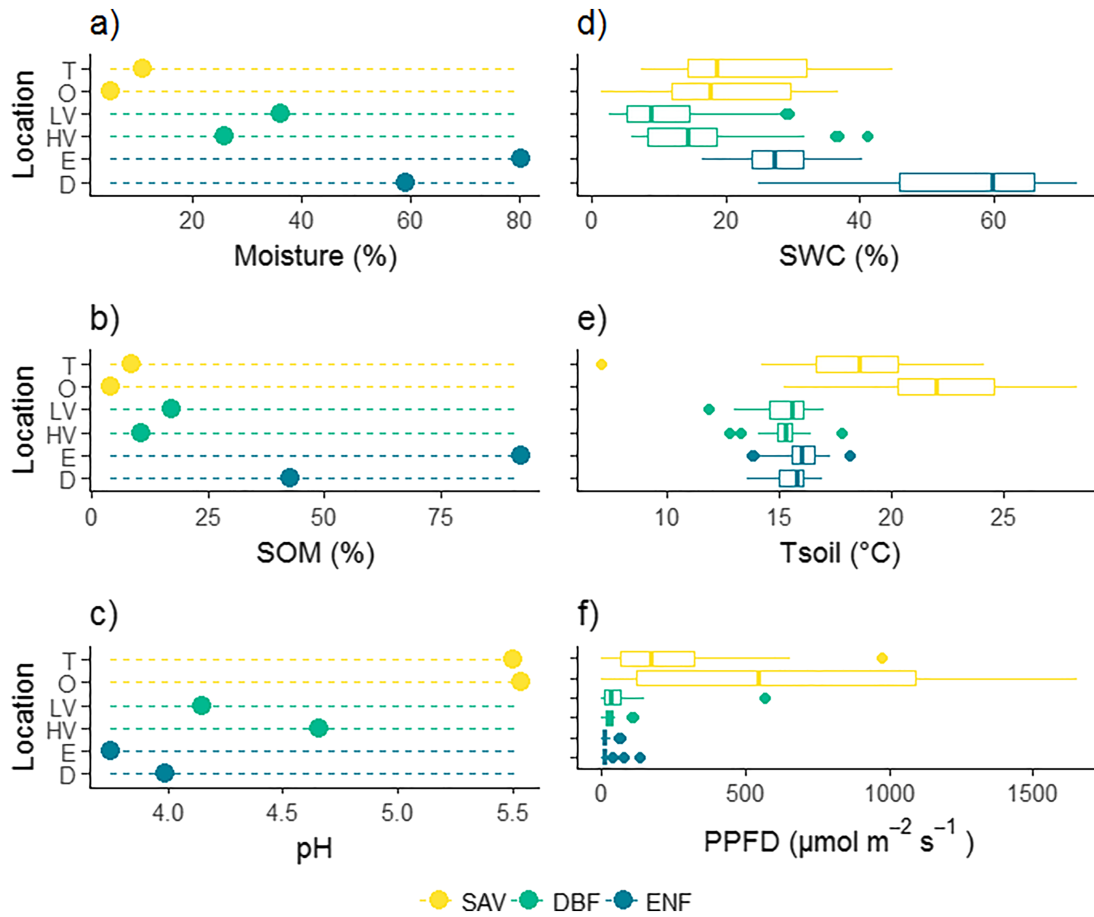


**Figure 1.** Summary of measured environmental parameters in the lab (a–c) and in the field (d–f).

$$F = \frac{q(C_2 - C_1)}{A} \quad (1)$$

$F$  denotes the soil flux in  $\text{pmol m}^{-2} \text{s}^{-1}$  for COS and  $\mu\text{mol m}^{-2} \text{s}^{-1}$  for  $\text{CO}_2$  (air temperature and pressure were measured to calculate the molar density),  $q$  is the flow rate (mol/s) while measuring the chamber concentrations,  $C_1$  is the ambient concentration derived from the linear interpolation ( $\text{pmol mol}^{-1}$  for COS and  $\mu\text{mol mol}^{-1}$  for  $\text{CO}_2$ ),  $C_2$  is the concentration in the chamber at steady state, and  $A$  is the surface area ( $0.032 \text{ m}^2$ ) covered by the chamber.

Differential pressure measurements (MKS Baratron Type 226A Differential Pressure Transducer, MKS Instruments Inc., Andover, MA, USA) were conducted with the same setup in Florian Kitz et al. (2017) to find the best flow rate, avoiding under inflation or overpressure within the chamber (Rayment & Jarvis, 1997). A flow rate of 1.55 standard liter (sl) per minute resulted in pressure differences being lower than 0.2 Pa, corresponding to the instrument resolution. Small COS emissions, with a maximum of  $2 \text{ pmol m}^{-2} \text{s}^{-1}$ , from the setup itself were reported by Florian Kitz et al. (2017).

### 2.3. Laboratory Measurements

Soil samples were taken at each study site as soil cores of the uppermost 10 cm of the soil profile and stored at  $-20^\circ\text{C}$ , a temperature where no changes in the microbial community composition can be expected (Lauber et al., 2010). The samples were sieved, with a mesh size of 2 mm, in preparation for the gas exchange measurements. To determine dry weight, a portion of each soil sample was oven dried at  $105^\circ\text{C}$  for at least 24 h and subsequently weighted. The pH was determined in soil:water extracts (1:5, w/v) by using a pH Meter

Metrohm 744 (Herisau, Switzerland). Total C and N contents were analyzed in dried samples, using a CN analyzer (TruSpec CHN; LECO, Michigan, USA) (supporting information Figure S3).

Soil samples were taken out of the freezer 24 h prior to measuring their gas exchange. They were filled into glass tubes with a diameter of 28 mm and a length of 150 mm. The glass tubes were connected to valves (Parker-Hannafin, Cleveland, OH, USA) switching between empty and filled, with soil, tubes every 5 min. The same instrument as used in situ, the Aerodyne Mini QCL, with the same settings was used for the lab measurements. Pressurized air was drawn into the QCL through water bottles, to humidify the air, and the glass tubes at a flow rate of 0.103 sl min<sup>-1</sup>. Fluxes were calculated with equation (2).

$$F = \frac{q(C_2 - C_1)}{g} \quad (2)$$

where  $F$  is the soil flux in pmol g<sup>-1</sup> s<sup>-1</sup> for COS and  $\mu\text{mol g}^{-1} \text{s}^{-1}$  for CO<sub>2</sub>,  $q$  is the flow rate (mol/s),  $C_1$  is the mean concentration of the empty tube measurements before and after the sample tube measurement (pmol mol<sup>-1</sup> and  $\mu\text{mol mol}^{-1}$ ),  $C_2$  is the concentration in the sample tube, and  $g$  is the soil fresh weight in grams. Blank measurements, with all tubes empty, were performed before the experiment started, and no contaminations were detected. The weight (g) used for each site and treatment varied to avoid huge volume differences, since soil with more organic material has a lower density compared to mineral soil. The system was given 1 hour to equilibrate for each set of measurements; data recorded during this period were discarded. Measurements were conducted in the dark, with aluminum foil covering the glass tubes, and under UV exposure. To expose the soil samples to UV radiation, a mercury vapor lamp (Actinic BL TL TL-K 40 W/10-R; Philips Lighting, Eindhoven, Netherlands), emitting primarily light between 350 and 400 nm with peak intensity at 370 nm, was used.

The programming language Python (Anaconda distribution, version 4.3.25) was used to calculate the fluxes and the “uncertainties” package (Lebigot n.d.) to propagate errors.

#### 2.4. Statistics

Statistical analyses were carried out with R version 4.5.0—“Joy in Playing” (R Core Team, 2018), RStudio (RStudio Team, 2016), and the package “data.table” (Dowle & Srinivasan, 2018). In preparation for all statistical analyses the respective data were investigated as described in Zuur et al. (2010). In case of a violation of homogeneity of residuals, robust sandwich errors (Zeileis, 2004), implemented in the “sandwich package,” were used. In the DBF only the data from chambers with litter were used, and one observation, identified as outlier, was excluded. The predictors (PPFD, Tsoil, and SWC) were centered when interactions were included in the linear model to reduce multicollinearity. The relative importance of the predictors for the soil COS flux was calculated using the relaimpo package (Grömping, 2006) with the method “lmg” (Lindeman et al., 1980). Kruskal-Wallis and Dunn’s tests were performed to test for significant differences between dark/light, night/day and sites. An analyses of variance (ANOVA) was performed for the laboratory measurements.

### 3. Results

#### 3.1. In Situ Measurements

Mean COS fluxes during daytime were highest in the SAV and lowest in the ENF, while nighttime COS fluxes were lowest in the DBF (Table 1). Mean in situ COS and CO<sub>2</sub> fluxes from the SAV were significantly different from the DBF ( $p$  value <0.001) and the ENF ( $p$  value <0.001) during daytime. Nighttime in situ COS fluxes from the SAV were significantly different from the DBF ( $p$  value <0.001) and the ENF ( $p$  value <0.001); CO<sub>2</sub> fluxes from the SAV were only significantly different from the DBF ( $p$  value <0.01). DBF and ENF in situ COS fluxes were significantly different from each other during the day ( $p$  value <0.001), but not during the night ( $p$  value >0.05), while in situ CO<sub>2</sub> fluxes of the two sites were significantly different during daytime and nighttime ( $p$  value <0.01).

No significant location or interaction effects were detected in the multiple linear regression for the SAV. In both the DBF and the ENF interaction effects with SWC were significant ( $p$  value <0.05) and were subsequently included in the final models (for interaction plots see Figure 2).



**Table 1**  
Mean COS and CO<sub>2</sub> fluxes (Mean ± SD) for the Lab and Field Experiments

| In situ    |  |  |  |             |
|------------|--|--|--|-------------|
| Site       | COS flux (pmol m <sup>-2</sup> s <sup>-1</sup> ) |  | CO <sub>2</sub> flux (μmol m <sup>-2</sup> s <sup>-1</sup> ) |             |
|            | Daytime  | Nighttime                                    | Daytime  | Nighttime   |
| SAV        | 5.8 ± 7.8  | 0.2 ± 1.5                                    | 6.5 ± 2.6  | 7.0 ± 2.2   |
| DBF        | -3.2 ± 3.7                                       | -4.6 ± 0.6                                   | 3.7 ± 1.4  | 2.6 ± 0.9   |
| ENF        | -3.5 ± 1.1                                       | -2.6 ± 0.9                                   | 9.3 ± 3.1  | 7.3 ± 2.8   |
| Laboratory |  |  |  |             |
|            | COS flux (pmol g <sup>-1</sup> s <sup>-1</sup> ) |  | CO <sub>2</sub> flux (nmol g <sup>-1</sup> s <sup>-1</sup> ) |             |
|            | Light  | Dark   | Light  | Dark        |
| SAV        | 5.4*10 <sup>-4</sup> ± 1.4*10 <sup>-4</sup>      | 2.4*10 <sup>-4</sup> ± 9.1*10 <sup>-5</sup>  | 0.03 ± 0.02  | 0.02 ± 0.01 |
| DBF        | -2.6*10 <sup>-4</sup> ± 7.0*10 <sup>-5</sup>     | -6.4*10 <sup>-4</sup> ± 6.7*10 <sup>-5</sup> | 0.05 ± 0.01  | 0.04 ± 0.01 |
| ENF        | -2.0*10 <sup>-5</sup> ± 1.7*10 <sup>-4</sup>     | -4.8*10 <sup>-4</sup> ± 6.6*10 <sup>-5</sup> | 0.08 ± 0.01  | 0.07 ± 0.01 |

For the simple SAV multiple linear regression  $\widehat{\text{COS flux}} = \hat{\beta}_0 + \hat{\beta}_1 \text{PAR} + \hat{\beta}_2 \text{Tsoil} + \hat{\beta}_3 \text{SWC}$  no multicollinearity (variance inflation factors < 4) was detected, and the whole model had predictive capability (F Statistic:  $p < 0.05$ ). Since the residuals were heteroscedastic, robust sandwich standard errors were used. For the SAV the multiple linear regression explained 74% of the variation in the response variable (COS flux) and the predictors PAR and Tsoil were highly significant ( $p$  value < 0.001). PAR was the most important predictor in the model followed by Tsoil (Figure 3). For the DBF multiple linear regression  $\widehat{\text{COS flux}} = \hat{\beta}_0 + \hat{\beta}_1 \text{PAR} + \hat{\beta}_2 \text{Tsoil} + \hat{\beta}_3 \text{SWC} + \hat{\beta}_4 \text{Location 2} + \hat{\beta}_5 \text{Location 3} + \hat{\beta}_6 (\text{PAR} * \text{Location 2}) + \hat{\beta}_7 (\text{PAR} * \text{Location 3}) + \hat{\beta}_8 (\text{SWC} * \text{Location 2}) + \hat{\beta}_9 (\text{SWC} * \text{Location 3}) + \hat{\beta}_{10} (\text{Tsoil} * \text{Location 2}) + \hat{\beta}_{11} (\text{Tsoil} * \text{Location 3})$  multicollinearity between the predictors and interactions including them was detected, and the whole model had predictive capability (F Statistic:  $p < 0.05$ ). The model explained 36% of the variation in the COS flux, Tsoil and interactions between the locations and SWC were significant ( $p$  value < 0.05). Tsoil was the most important predictor in the model (Figure 3). For the ENF multiple linear regression  $\widehat{\text{COS flux}} = \hat{\beta}_0 + \hat{\beta}_1 \text{PAR} + \hat{\beta}_2 \text{Tsoil} +$

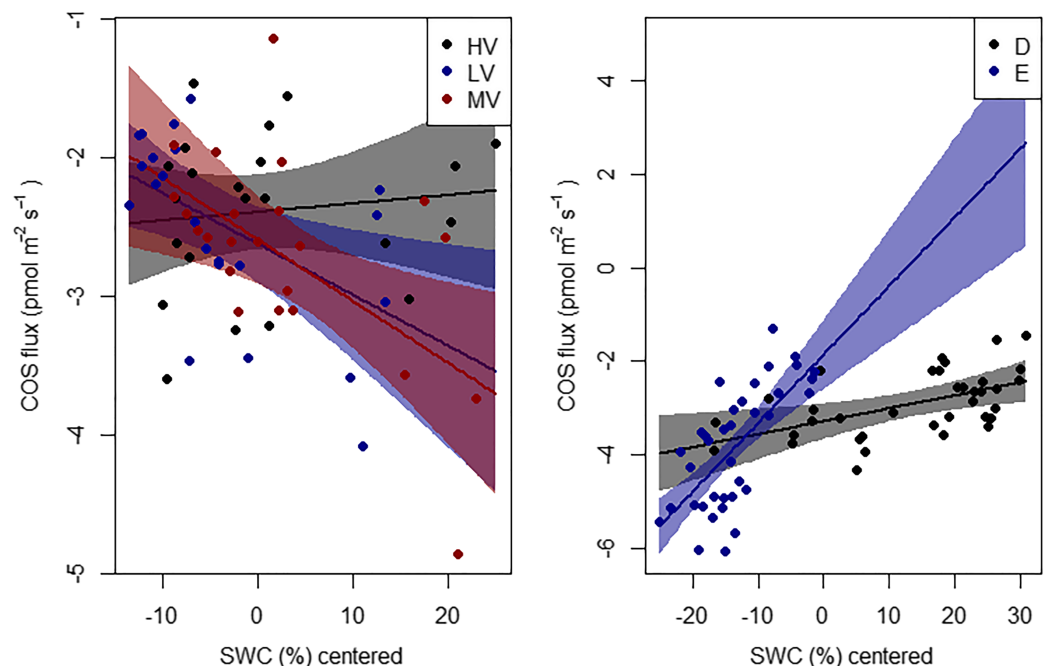


**Figure 2.** Interaction plots for the interactions SWC \* Location in the DBF (a) and the ENF (b) as included in the multiple linear regression models described in the text.

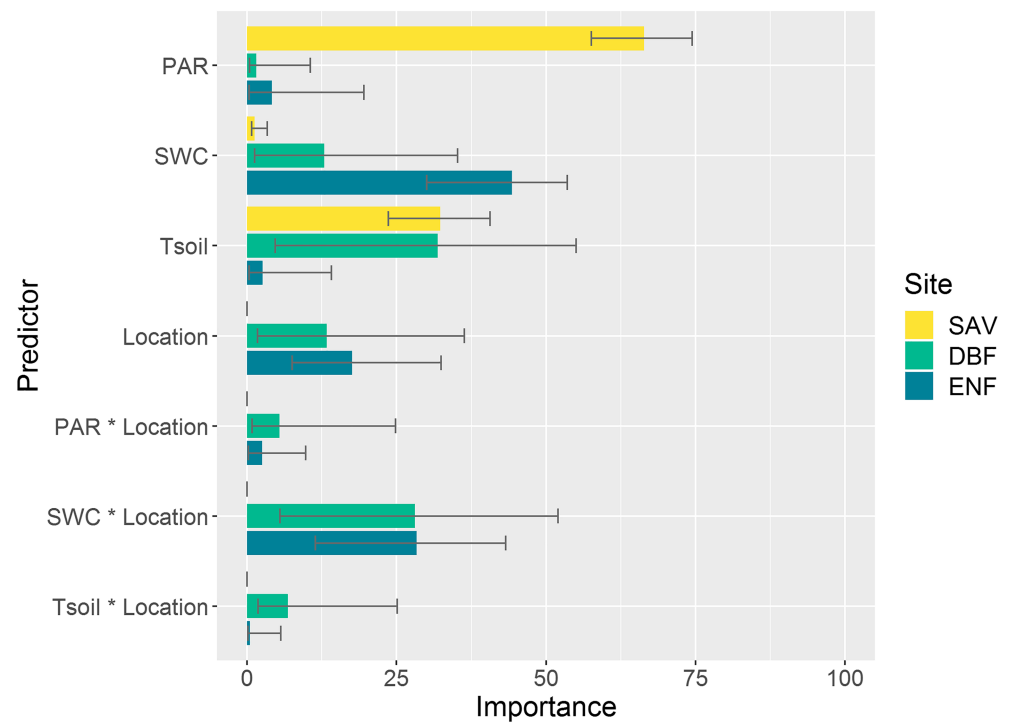


**Figure 3.** Relative importance of the predictors in the multiple linear regressions discussed in the results section. The relative importance is normalized to  $R^2$ , always summing up to 100. Produced by the relaimpo package.

$\hat{\beta}_3$ SWC +  $\hat{\beta}_4$ Location 2 +  $\hat{\beta}_5$ (PAR\*Location 2) +  $\hat{\beta}_6$ (SWC\*Location 2) +  $\hat{\beta}_7$ (Tsoil\*Location 2) multicollinearity between the predictors and interactions including them was detected, and the whole model had predictive capability (F Statistic:  $p < 0.05$ ). The model explained 55% of the variation in the COS flux. SWC, location, and interactions between the locations and SWC were significant ( $p$  values  $< 0.05$ ). SWC was the most important predictor in the model followed by the interaction between SWC and location (Figure 3). Coefficients and standard errors for the linear models are summarized in Table 2.

### 3.2. Laboratory Incubations

Mean COS fluxes were highest in the SAV and lowest in the DBF, both in the dark and under UV radiation (Table 1). All three sites were significantly different ( $p < 0.001$ ) to each other in their COS and  $\text{CO}_2$  flux means.

Mean COS fluxes from SAV soil samples were significantly different between samples collected under the tree and in the open and between the dark and light treatment (see ANOVA summary in Table 3). There was also a significant interaction between those two factors (see ANOVA results, Table 3).  $\text{CO}_2$  fluxes were significantly different between the SAV sampling locations and between the dark and light exposed samples, but there was no significant interaction. Mean COS fluxes from DBF soil samples were significantly different between samples collected in differently dense vegetated areas and between the dark and light treatment applied in the lab (see ANOVA results, Table 3). There was no significant interaction between the factors (see ANOVA results, Table 3).  $\text{CO}_2$  fluxes were significantly different between DBF sampling locations and between the dark and light exposed samples. There was also a significant interaction effect between the sample location and dark/light exposure. Mean COS fluxes from ENF soil samples were significantly different between samples collected at the elevation and in the depression and between the dark and light treatment applied in the lab (see ANOVA results, Table 3). There was also a significant interaction between those two factors (see ANOVA results, Table 3).  $\text{CO}_2$  fluxes were significantly different between ENF sampling locations and between the dark and light exposed samples, but the interaction was not significant. The COS/ $\text{CO}_2$  ratio was significantly different between locations and dark/light treatments in samples from all

**Table 2**  
Summary Statistics for the Multiple Linear Regressions Discussed in the Results Section

| Predictor          | SAV                     |            | DBF                    |            | ENF                      |            |
|--------------------|-------------------------|------------|------------------------|------------|--------------------------|------------|
|                    | Estimate                | Std. error | Estimate               | Std. error | Estimate                 | Std. error |
| Intercept          | 1.59E+01 <sup>***</sup> | 2.62E+01   | -2.38 <sup>*</sup>     | 1.30E-01   | -2.57E+00 <sup>***</sup> | 2.10E-01   |
| PAR                | 9.57E-03 <sup>***</sup> | 7.32E-04   | -2.21E-03              | 5.00E-03   | -6.20E-03                | 5.78E-03   |
| SWC                | 1.58E-02                | 3.79E-02   | 6.11E-03               | 1.34E-02   | 8.73E-02 <sup>***</sup>  | 1.35E-02   |
| Tsoil              | 7.59E-01 <sup>***</sup> | 1.12E-01   | 3.27E-01 <sup>*</sup>  | 1.50E-01   | 9.29E-02                 | 1.15E-01   |
| Location 2         |                         |            | -2.63E-01              | 1.92E-01   | 7.17E-01 <sup>**</sup>   | 2.12E-01   |
| Location 3         |                         |            | -1.76E-01              | 1.96E-01   |                          |            |
| PAR * location 2   |                         |            | 4.31E-03               | 6.31E-03   | -2.37E-03                | 5.78E-03   |
| PAR * location 3   |                         |            | -3.62E-03              | 7.31E-03   |                          |            |
| SWC * location 2   |                         |            | -4.28E-02 <sup>*</sup> | 1.99E-02   | 5.96E-02 <sup>***</sup>  | 1.35E-02   |
| SWC * location 3   |                         |            | -5.06E-02 <sup>*</sup> | 2.14E-02   |                          |            |
| Tsoil * location 2 |                         |            | -1.76E-01              | 1.94E-01   | 1.24E-02                 | 1.15E-01   |
| Tsoil * location 3 |                         |            | 4.33E-02               | 2.13E-01   |                          |            |
| Observations       | 140                     |            | 67                     |            | 72                       |            |
| R <sup>2</sup>     | 0.74                    |            | 0.36                   |            | 0.55                     |            |

Note. Location 2 corresponds to LV in the DBF and E in the ENF. Location 3 corresponds to MV in the DBF. The intercepts for DBF and ENF have to be treated with caution, since the predictors were centered. Significance levels: \*\*\*  $p < 0.001$ , \*\*  $p < 0.01$ , \*  $p < 0.05$ .

three sites (SAV, DBF, and ENF). The mean difference in the COS flux between light and dark treatment correlated with the soil organic matter (SOM) content of the soil samples. Samples with higher SOM content had a higher mean difference between the treatments (e.g., the difference in the COS flux between the light and dark treatment was higher) compared to samples with lower SOM content, even across sites, with the exception of the ENF depression samples (see supporting information Figure S4).

#### 4. Discussion

A recent synthesis paper (Whelan et al., 2018) summarized soil COS fluxes from a multitude of different studies and ecosystems with a majority of reported COS uptake in oxic soils in the range of  $-10$  to  $0$   $\text{pmol m}^{-2} \text{s}^{-1}$ . Our in situ measurements of soil COS fluxes in both forest ecosystems (DBF and ENF), in Denmark and Estonia, were well in this range (Figure 4). The oak savannah (SAV) in Spain though was characterized by

very high positive soil COS fluxes (Figure 4), especially in the open grass during daytime, exceeding most values found in the literature (Whelan et al., 2018). These high fluxes correlate with high light intensities on the soil surface, favored by the removal of the above-ground vegetation in the chambers, which would otherwise provide shading. In order to estimate the surface COS fluxes in the SAV under natural conditions, hence with intact vegetation, and to put it into perspective with the measured fluxes, the linear model (Table 2), driven by an estimate of the PPFD at the soil surface based on the Beer-Lambert law (Campbell & Norman, 1998), can be used. A measured PPFD of  $2,191 \mu\text{mol m}^{-2} \text{s}^{-1}$ , the maximum observed at this site, would equate to  $693.8 \mu\text{mol m}^{-2} \text{s}^{-1}$  if shading by the vegetation, with a mean leaf area index (LAI) of 2.3 (calculated from the removed biomass) and an estimated extinction coefficient of 0.5 (Zhang et al., 2014), was factored in. Plugging in the derived PPFD into the linear model (Table 2), with a soil temperature of  $25^\circ\text{C}$  and a SWC of 18%, would yield a soil COS flux of  $10.03 \text{ pmol m}^{-2} \text{ s}^{-1}$  under maximum light conditions but with shading by the vegetation, still a high value but comparable to COS fluxes measured by Maseyk et al. (2014) or Florian Kitz et al. (2017).

**Table 3**  
Summary of the ANOVA Results

|               | DF  | SS       | F value | P value                   |
|---------------|-----|----------|---------|---------------------------|
| SAV           |     |          |         |                           |
| Location      | 1   | 2.46E-06 | 1050.3  | $< 2e-16$ <sup>***</sup>  |
| UV            | 1   | 5.46E-06 | 2334.2  | $< 2e-16$ <sup>***</sup>  |
| Location * UV | 1   | 9.20E-08 | 39.4    | $1.76E-09$ <sup>***</sup> |
| Residuals     | 224 | 5.24E-07 |         |                           |
| DBF           |     |          |         |                           |
| Location      | 1   | 2.90E-07 | 94      | $< 2e-16$ <sup>***</sup>  |
| UV            | 1   | 8.28E-06 | 2396.7  | $< 2e-16$ <sup>***</sup>  |
| Location * UV | 1   | 0.00E+00 | 0.001   | $9.70E-01$                |
| Residuals     | 224 | 7.74E-07 |         |                           |
| ENF           |     |          |         |                           |
| Location      | 1   | 1.12E-06 | 175.1   | $< 2e-16$ <sup>***</sup>  |
| UV            | 1   | 1.22E-05 | 1927.8  | $< 2e-16$ <sup>***</sup>  |
| Location * UV | 1   | 1.17E-06 | 184.3   | $< 2e-16$ <sup>***</sup>  |
| Residuals     | 224 | 1.42E-06 |         |                           |

Note. DF = degrees of freedom; SS = sum of squares. \*\*\*  $p < 0.001$ , \*\*  $p < 0.01$ , \*  $p < 0.051$ .



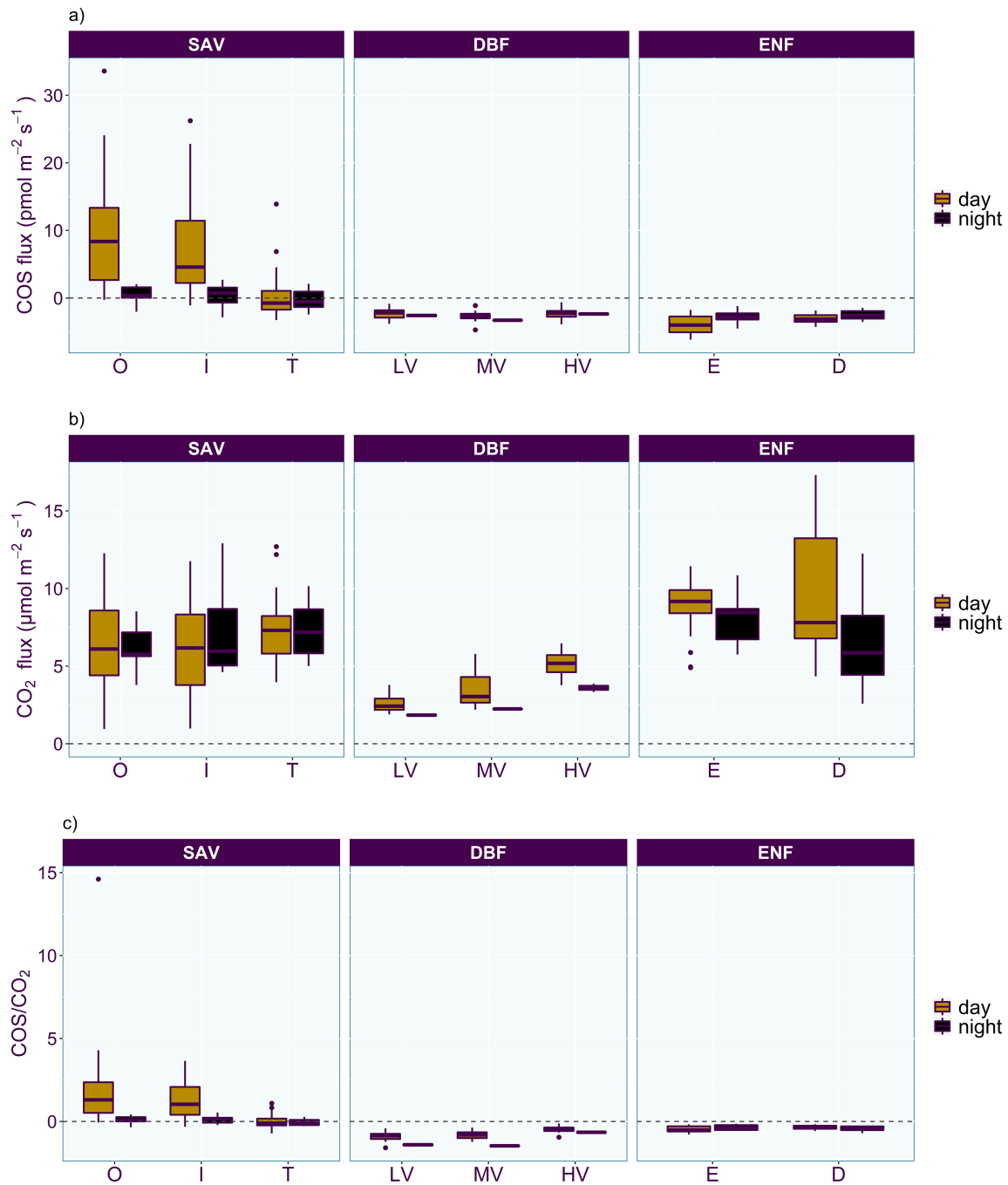


**Figure 4.**  $\text{CO}_2$  (a) and COS (b) fluxes measured in situ in the savannah (SAV) in Spain, the deciduous broadleaf forest (DBF) in Denmark, and the evergreen needleleaf forest (ENF) in Estonia. Colors denote the location within the ecosystems, with under the Tree (T), open savannah (O), and intermediate (I) in the SAV, low (LV), medium (MV), and high vegetation (HV) surrounding the rings in the DBF and elevation (E) and depression (D) in the ENF. (c) The ratio of the COS and  $\text{CO}_2$  flux.

The linear regression confirms that the COS flux in the SAV was primarily driven by radiation, as indicated by PPFd being the most important predictor, explaining 66% of the variability in the observed surface COS flux. In the two denser forest sites (DBF and ENF) in Denmark and Estonia PPFd was not a good explanatory variable for the in situ soil COS flux, most likely due to a very narrow range of PPFd on the soil surface and low light levels (DBF:  $44.4 \pm 74 \mu\text{mol m}^{-2} \text{s}^{-1}$ ; ENF:  $18.9 \pm 21.2 \mu\text{mol m}^{-2} \text{s}^{-1}$ ) in general. But as it can be seen in the no litter chambers in the DBF, sunlight penetrating the forest canopy for a short period of time

can lead also in this ecosystem to a strong response in the soil COS flux (supporting information Figure S1). The strong light response of the soil COS flux was also seen in the lab, where all soil samples showed a strong reaction to UV-A exposure (Figure 5 and supporting information Figure S5), especially remarkable was the strong intrasite variability (Figure 5). Whelan and Rhew (2015), who exposed their soil samples to visible light, also saw an increase of COS production under light exposure, even in sterilized soil samples, a response that increased even more when roots were kept in the soil. Our samples exhibited a comparable behavior, samples with higher soil organic matter content usually exhibiting a stronger reaction to light (see supporting information Figure S4), which holds true within and between sites, with the exception of samples from the ENF depression (Figures 5 and 1). The effect of radiation on organic material is understood to be complex (King et al., 2012) and can vary with identity, for example, chemical composition, and age of the substrate (Austin et al., 2016; Day et al., 2015; Gallo et al., 2009). SOM and its decomposability can vary greatly in soils (Marschner et al., 2008) depending on the composition of organic input to the soil system (Kögel-Knabner, 2002) and interactions with mineral components of the soil (Marschner et al., 2008; Mikutta et al., 2006), but knowledge about its chemical and physical properties is limited (Dungait et al., 2012; Hedges et al., 2000). Meredith et al. (2018) showed that the soil sulfur species composition can vary greatly in soils, which in turn impacts COS production. In their study they were able to link higher sulfate concentrations to increased COS production. The question whether the source of the soil COS emission under light exposure is primarily abiotic or biotic is difficult to investigate, since the experimental setup was not designed to distinguish between facilitation of microbial decomposition (Lin et al., 2018), through photo-priming, and direct abiotic destruction of organic material by radiation. Previous studies (F. Kitz et al., 2019; Meredith et al., 2018) hypothesized that COS production is caused by coupled abiotic and biotic processes, with biotic processes often providing the precursors from which COS is produced abiotically. With the absence of high light levels as a driving factor in DBF and ENF other parameters gained importance in explaining the in situ variability, but the overall explained variance by the linear models decreased substantially (Table 2). In DBF soil temperature was the factor best explaining the observed variability in the soil COS fluxes (Figure 3) but not so in SAV. The soil temperature range in DBF and ENF was too narrow to investigate an optimum curve, indicating temperature-dependent biological activity with an optimum for biological COS uptake, as proposed by Kesselmeier et al. (1999), while in SAV COS emissions increased linearly with soil temperature, indicating primarily abiotic processes, a response reported previously in the literature (Maseyk et al., 2014; Whelan et al., 2016; Whelan & Rhew, 2015). When soil temperature increased at the SAV site, soil CO<sub>2</sub> fluxes increased as well. The soil CO<sub>2</sub> flux can serve as an estimator for biological activity in the soil and litter layer, since it primarily originates from respiration processes (Hanson et al., 2000; Insam & Haselwandter, 1989; Jensen et al., 1996). The increase in CO<sub>2</sub> emissions in SAV therefore indicates an increase in biological activity in the soil with increasing temperature, a common but very variable response of soils observed in many different ecosystems (Conant et al., 2011; Davidson et al., 1998; Davidson & Janssens, 2006; Jensen et al., 1996; Lloyd & Taylor, 1994). Since there are more accounts for biotic COS consumption (Kato et al., 2008; Kato et al., 2012; Kesselmeier et al., 1999; Masaki et al., 2016; Ogawa et al., 2013; Ogawa et al., 2016; Sauze et al., 2017) than biotic COS production (Conrad, 1996; Masaki et al., 2016) under ambient COS concentrations, it is tempting to link biological activity in oxic soils primarily to COS uptake. The co-occurring increase in COS and CO<sub>2</sub> emissions in SAV could therefore mean that abiotic production of COS is increasing more strongly with temperature outweighing increased COS uptake due to higher biological activity or the underlying assumption of biotic COS contribution being primarily characterized by COS uptake in oxic soils is not universally true, and emissions associated to the soil biological activity could also occur.

Another parameter, which is connected to microbial activity and is considered to have a decisive influence on soil COS fluxes, is the soil water content (Bunk et al., 2017; Kesselmeier et al., 1999; Ogee et al., 2016; Van Diest & Kesselmeier, 2008). Soil COS uptake is expected to exhibit a bell-shaped curve along a SWC gradient (Kesselmeier et al., 1999; Van Diest & Kesselmeier, 2008), with a reduction of soil COS uptake at low SWC, due to reduced microbial and enzyme activity (Borken & Matzner, 2009; Davidson & Janssens, 2006; Lavigne et al., 2004; Sardans & Penuelas, 2005) caused by water limitation, and reduced diffusivity of COS in the soil column at high SWC (Ogee et al., 2016; Sun et al., 2015). Even though our in situ measurements cover a wide range of SWC (Figure 1) the impact of soil moisture is difficult to separate from associated soil parameters, like soil organic matter content, which has to be kept in mind when evaluating the SWC contribution to the linear models. In the two wetter ecosystems, DBF and ENF, the interaction between SWC and location was

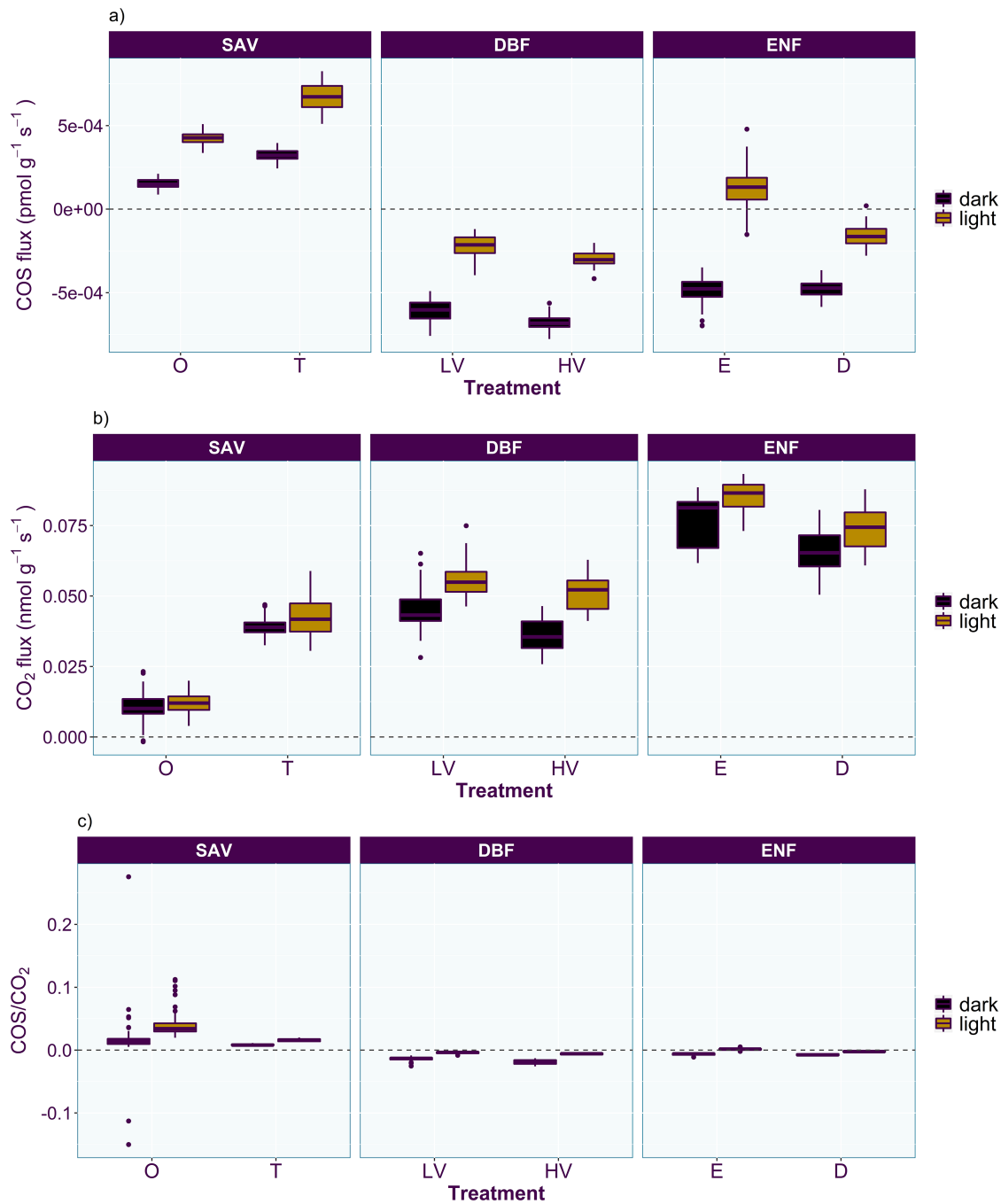


**Figure 5.** COS (a) and CO<sub>2</sub> (b) fluxes measured in the laboratory from SAV, DBF, and ENF soil samples. Colors denote the sampling location within the ecosystems, with under the Tree (T) and open savannah (O) in the SAV, low (LV) and high vegetation (HV) surrounding the rings in the DBF and elevation (E) and depression (D) in the ENF. “light” indicates soil samples exposed to UV radiation. (c) The ratio of the COS and CO<sub>2</sub> flux.

significant, which complicates the interpretation of the main effect, SWC, in the model (Irwin & McClelland, 2001; McClelland & Judd, 1993). But if we investigate the SWC impact on soil COS fluxes in the different locations separately (Figure 2), a decrease in COS uptake with increasing SWC in ENF and the reverse in DBF is observed. A striking phenomenon is the strong intrasite variability, which is likely caused by the large differences in soil properties (Figure 1) within the sites, especially in ENF. This suggests that the response of the soil COS flux to changing SWC is very variable and depends greatly on soil and litter layer (Sun et al., 2016) properties.

Soil COS fluxes in the laboratory, in the dark and under the same temperature conditions, did also vary between soil samples from the different sites. Such variability between different soils under laboratory conditions was observed previously (Bunk et al., 2017; Kaisermann, Ogée, et al., 2018; Meredith et al., 2018; Meredith et al., 2019; Whelan et al., 2016); notable in our experiment is the consistently positive COS flux from the SAV soil. Positive soil COS fluxes were rarely observed in untreated soil samples in previous laboratory studies. In the few experiments where COS emission were detected (Bunk et al., 2017; Whelan et al., 2016), the corresponding soil samples were very dry, as with the SAV samples (Figure 1). Other soil parameters, found to influence the soil COS exchange in the literature, are soil pH (Sauze et al., 2017) and soil nitrogen content (Kaisermann, Jones, et al., 2018; Meredith et al., 2018). Soil pH differed between our samples (Figure 1) with COS uptake in the more acidic samples and COS production in the less acidic samples, while no apparent pattern emerged from the C/N ratio of our samples with regard to soil COS fluxes (supporting information Figure S3).

## 5. Conclusions

Our approach to complement field with laboratory measurements allowed us to address the three formulated hypotheses under in situ and controlled conditions. From both the field and laboratory measurements, radiation emerged as the most impactful driver for the soil COS flux, confirming hypothesis (I). But in ecosystems with low light levels on the soil surface, like in dense forests, the importance of radiation for in situ soil COS flux was reduced, despite its potential impact seen in the lab. In situ, intersite variability in soil COS fluxes, as proposed in hypothesis (II), was observed in the forest sites, DBF and ENF, and the savannah. And while in situ measurements did not reveal a significant difference in the mean of the soil COS flux between the forests, laboratory measurements did, probably originating from the differences between soil samples in the lab and natural soils with a developed litter layer and living roots. Most surprising to us was the large intrasite variability, hypothesis (III), in both in situ and laboratory measurements, which did also change the response to UV radiation. We suspect especially the amount and chemical composition of soil organic matter to be of great importance for explaining the observed differences in the light response and the overall differences within and between sites. It is important to note that while we have separated parameters, like SWC and SOM, in analyses and discussion, they are of course related to each other (Ankenbauer & Loheide, 2017) and indivisible in situ. Among the biggest obstacles we currently face in explaining soil COS fluxes is our lack of understanding for the basic chemical processes leading to COS emissions. Future studies should therefore explore the effect of environmental parameters, especially radiation, on organic matter in the soil and on the soil surface and their interactions with biological decomposition processes.

## Acknowledgments

This study was financially supported by the Austrian National Science Fund (FWF) under contracts P27176-B16 and P31669-B22, and the Tyrolean Science Fund (TWF) under contract UNI-0404/1801. Thanks to Andreas Brændholt, Herbert Wachter, Mario Deutschmann, Katharina Gerdel, the Institute of Atmospheric and Cryospheric Sciences, and the Institute for Microbiology of the University of Innsbruck. Financial support was further granted by the Ministry of Education and Research of Estonia (basal funding grants P170026 and P18002); the Estonian Research Infrastructures Roadmap project Estonian Environmental Observatory (3.2.0304.11-0395); the European Commission by ERA-NET-Cofund action ERA\_PLANET (689443), the Centre of Excellence EcolChange; and the European Social Fund (Mobilitas postdoctoral grant MJD 257). We thank Beate Noe for the processing of the litter samples at SMEAR Estonia. Data used in this manuscript can be found at 10.5281/zenodo.3664784.

## References

- Ankenbauer, K. J., & Loheide, S. P. (2017). The effects of soil organic matter on soil water retention and plant water use in a meadow of the Sierra Nevada, CA. *Hydrological Processes*, *31*(4), 891–901. <https://doi.org/10.1002/hyp.11070>
- Austin, A. T., Mendez, M. S., & Ballare, C. L. (2016). Photodegradation alleviates the lignin bottleneck for carbon turnover in terrestrial ecosystems. *Proceedings of the National Academy of Sciences of the United States of America*, *113*(16), 4392–4397. <https://doi.org/10.1073/pnas.1516157113>
- Berkelhammer, M., Asaf, D., Still, C., Montzka, S., Noone, D., Gupta, M., et al. (2014). Constraining surface carbon fluxes using in situ measurements of carbonyl sulfide and carbon dioxide. *Global Biogeochemical Cycles*, *28*, 161–179. <https://doi.org/10.1002/2013gb004644>
- Berry, J., Wolf, A., Campbell, J. E., Baker, I., Blake, N., Blake, D., et al. (2013). A coupled model of the global cycles of carbonyl sulfide and CO<sub>2</sub>: A possible new window on the carbon cycle. *Journal of Geophysical Research: Biogeosciences*, *118*, 842–852. <https://doi.org/10.1002/jgrg.20068>
- Borken, W., & Matzner, E. (2009). Reappraisal of drying and wetting effects on C and N mineralization and fluxes in soils. *Global Change Biology*, *15*(4), 808–824. <https://doi.org/10.1111/j.1365-2486.2008.01681.x>
- Bunk, R., Behrendt, T., Yi, Z. G., Andraea, M. O., & Kesselmeier, J. (2017). Exchange of carbonyl sulfide (OCS) between soils and atmosphere under various CO<sub>2</sub> concentrations. *Journal of Geophysical Research: Biogeosciences*, *122*, 1343–1358. <https://doi.org/10.1002/2016jg003678>
- Campbell, G. S., & Norman, J. M. (1998). *An Introduction to Environmental Biophysics*, (2nd ed.). New York: Springer.
- Conant, R. T., Ryan, M. G., Ågren, G. I., Birge, H. E., Davidson, E. A., Eliasson, P. E., et al. (2011). Temperature and soil organic matter decomposition rates—Synthesis of current knowledge and a way forward. *Global Change Biology*, *17*(11), 3392–3404. <https://doi.org/10.1111/j.1365-2486.2011.02496.x>
- Conrad, R. (1996). Soil microorganisms as controllers of atmospheric trace gases (H<sub>2</sub>, CO, CH<sub>4</sub>, OCS, N<sub>2</sub>O, and NO). *Microbiological Reviews*, *60*(4), 609–640.
- Davidson, E. A., Belk, E., & Boone, R. D. (1998). Soil water content and temperature as independent or confounded factors controlling soil respiration in a temperate mixed hardwood forest. *Global Change Biology*, *4*(2), 217–227. <https://doi.org/10.1046/j.1365-2486.1998.00128.x>

- Davidson, E. A., & Janssens, I. A. (2006). Temperature sensitivity of soil carbon decomposition and feedbacks to climate change. *Nature*, *440*(7081), 165–173. <https://doi.org/10.1038/nature04514>
- Day, T. A., Guenon, R., & Ruhland, C. T. (2015). Photodegradation of plant litter in the Sonoran Desert varies by litter type and age. *Soil Biology & Biochemistry*, *89*, 109–122. <https://doi.org/10.1016/j.soilbio.2015.06.029>
- Dowle, M., & Srinivasan, A. (2018). data.table: Extension of 'data.frame'. (Version R package version 1.11.4). Retrieved from <https://CRAN.R-project.org/package=data.table>
- Du, Q. Q., Mu, Y. J., Zhang, C. L., Liu, J. F., Zhang, Y. Y., & Liu, C. T. (2017). Photochemical production of carbonyl sulfide, carbon disulfide and dimethyl sulfide in a lake water. *Journal of Environmental Sciences*, *51*, 146–156. <https://doi.org/10.1016/j.jes.2016.08.006>
- Dungait, J. A. J., Hopkins, D. W., Gregory, A. S., & Whitmore, A. P. (2012). Soil organic matter turnover is governed by accessibility not recalcitrance. *Global Change Biology*, *18*(6), 1781–1796. <https://doi.org/10.1111/j.1365-2486.2012.02665.x>
- Ensign, S. A. (1995). Reactivity of carbon-monoxide dehydrogenase from *rhodospirillum-rubrum* with carbon-dioxide, carbonyl sulfide, and carbon-disulfide. *Biochemistry*, *34*(16), 5372–5378. <https://doi.org/10.1021/bi00016a008>
- Gallo, M. E., Porrás-Alfaro, A., Odenbach, K. J., & Sinsabaugh, R. L. (2009). Photoacceleration of plant litter decomposition in an arid environment. *Soil Biology & Biochemistry*, *41*(7), 1433–1441. <https://doi.org/10.1016/j.soilbio.2009.03.025>
- Grömping, U. (2006). Relative importance for linear regression in R: The Package relaimpo. *Journal of Statistical Software*, *17*(1), 1–27.
- Hanson, P. J., Edwards, N. T., Garten, C. T., & Andrews, J. A. (2000). Separating root and soil microbial contributions to soil respiration: A review of methods and observations. *Biogeochemistry*, *48*(1), 115–146. <https://doi.org/10.1023/a:1006244819642>
- Hedges, J. I., Eglinton, G., Hatcher, P. G., Kirchman, D. L., Arnosti, C., Derenne, S., et al. (2000). The molecularly-uncharacterized component of nonliving organic matter in natural environments. *Organic Geochemistry*, *31*(10), 945–958. [https://doi.org/10.1016/S0146-6380\(00\)00096-6](https://doi.org/10.1016/S0146-6380(00)00096-6)
- Insam, H., & Haselwandter, K. (1989). Metabolic quotient of the soil microflora in relation to plant succession. *Oecologia*, *79*(2), 174–178. <https://doi.org/10.1007/bf00388474>
- Irwin, J. R., & McClelland, G. H. (2001). Misleading heuristics and moderated multiple regression models. *Journal of Marketing Research*, *38*(1), 100–109. <https://doi.org/10.1509/jmkr.38.1.100.18835>
- IUSS Working Group WRB (2006). *World reference base for soil resources 2006—A framework for international classification, correlation and communication*. Rome: Food and Agriculture Organization of the United Nations.
- Jensen, L. S., Mueller, T., Tate, K. R., Ross, D. J., Magid, J., & Nielsen, N. E. (1996). Soil surface CO<sub>2</sub> flux as an index of soil respiration in situ: A comparison of two chamber methods. *Soil Biology & Biochemistry*, *28*(10–11), 1297–1306. [https://doi.org/10.1016/s0038-0717\(96\)00136-8](https://doi.org/10.1016/s0038-0717(96)00136-8)
- Kaisermann, A., Jones, S., Wohl, S., Ogée, J., & Wingate, L. (2018). Nitrogen fertilization reduces the capacity of soils to take up atmospheric carbonyl sulphide. *Soil Systems*, *2*(4), 18. <https://doi.org/10.3390/soilsystems2040062>
- Kaisermann, A., Ogée, J., Sauze, J., Wohl, S., Jones, S. P., Gutierrez, A., & Wingate, L. (2018). Disentangling the rates of carbonyl sulphide (COS) production and consumption and their dependency with soil properties across biomes and land use types. *Atmospheric Chemistry and Physics Discussions*, *2018*, 1–27. <https://doi.org/10.5194/acp-2017-1229>
- Kato, H., Igarashi, Y., Dokiya, Y., & Katayama, Y. (2012). Vertical distribution of carbonyl sulfide at Mt. Fuji, Japan. *Water, Air, and Soil Pollution*, *223*(1), 159–167. <https://doi.org/10.1007/s11270-011-0847-0>
- Kato, H., Saito, M., Nagahata, Y., & Katayama, Y. (2008). Degradation of ambient carbonyl sulfide by *Mycobacterium* spp. in soil. *Microbiology*, *154*(Pt 1), 249–255. <https://doi.org/10.1099/mic.0.2007/011213-0>
- Kesselmeier, J., Teusch, N., & Kuhn, U. (1999). Controlling variables for the uptake of atmospheric carbonyl sulfide by soil. *Journal of Geophysical Research*, *104*(D9), 11577. <https://doi.org/10.1029/1999jd900090>
- Kettle, A. J., Kuhn, U., von Hobe, M., Kesselmeier, J., & Andreae, M. O. (2002). Global budget of atmospheric carbonyl sulfide: Temporal and spatial variations of the dominant sources and sinks. *Journal of Geophysical Research-Atmospheres*, *107*(D22). <https://doi.org/10.1029/2002jd002187>
- King, J. Y., Brandt, L. A., & Adair, E. C. (2012). Shedding light on plant litter decomposition: advances, implications and new directions in understanding the role of photodegradation. *Biogeochemistry*, *111*(1–3), 57–81. <https://doi.org/10.1007/s10533-012-9737-9>
- Kitz, F., Gerdel, K., Hammerle, A., Laterza, T., Spielmann, F. M., & Wohlfahrt, G. (2017). In situ soil COS exchange of a temperate mountain grassland under simulated drought. *Oecologia*, *183*(3), 851–860. <https://doi.org/10.1007/s00442-016-3805-0>
- Kitz, F., Gómez-Brandón, M., Eder, B., Etemadi, M., Spielmann, F. M., Hammerle, A., et al. (2019). Soil carbonyl sulfide exchange in relation to microbial community composition: Insights from a managed grassland soil amendment experiment. *Soil Biology & Biochemistry*, *135*, 28–37. <https://doi.org/10.1016/j.soilbio.2019.04.005>
- Kögel-Knabner, I. (2002). The macromolecular organic composition of plant and microbial residues as inputs to soil organic matter. *Soil Biology and Biochemistry*, *34*(2), 139–162. [https://doi.org/10.1016/S0038-0717\(01\)00158-4](https://doi.org/10.1016/S0038-0717(01)00158-4)
- Lauber, C. L., Zhou, N., Gordon, J. I., Knight, R., & Fierer, N. (2010). Effect of storage conditions on the assessment of bacterial community structure in soil and human-associated samples. *FEMS Microbiology Letters*, *307*(1), 80–86. <https://doi.org/10.1111/j.1574-6968.2010.01965.x>
- Launois, T., Peylin, P., Belviso, S., & Poulter, B. (2015). A new model of the global biogeochemical cycle of carbonyl sulfide—Part 2: Use of carbonyl sulfide to constrain gross primary productivity in current vegetation models. *Atmospheric Chemistry and Physics*, *15*(16), 9285–9312. <https://doi.org/10.5194/acp-15-9285-2015>
- Lavigne, M. B., Foster, R. J., & Goodine, G. (2004). Seasonal and annual changes in soil respiration in relation to soil temperature, water potential and trenching. *Tree Physiology*, *24*(4), 415–424.
- Lebigot, E. O. Uncertainties: A Python package for calculations with uncertainties (Version 2.4.6.1). Retrieved from <http://pythonhosted.org/uncertainties/>
- Li, G. Y., Mu, J. P., Liu, Y. Z., Smith, N. G., & Sun, S. C. (2017). Effect of microtopography on soil respiration in an alpine meadow of the Qinghai-Tibetan plateau. *Plant and Soil*, *421*(1–2), 147–155. <https://doi.org/10.1007/s11104-017-3448-x>
- Lin, Y., Karlen, S. D., Ralph, J., & King, J. Y. (2018). Short-term facilitation of microbial litter decomposition by ultraviolet radiation. *Science of the Total Environment*, *615*, 838–848. <https://doi.org/10.1016/j.scitotenv.2017.09.239>
- Lindeman, R. H., Merenda, P. F., & Gold, R. Z. (1980). *Introduction to bivariate and multivariate analysis*. Glenview, Illinois, United States: Scott Foresman.
- Liu, J., Geng, C., Mu, Y., Zhang, Y., Xu, Z., & Wu, H. (2010). Exchange of carbonyl sulfide (COS) between the atmosphere and various soils in China. *Biogeosciences*, *7*(2), 753–762. <https://doi.org/10.5194/bg-7-753-2010>
- Lloyd, J., & Taylor, J. A. (1994). On the temperature-dependence of soil respiration. *Functional Ecology*, *8*(3), 315–323. <https://doi.org/10.2307/2389824>



- Lopez-Sangil, L., Rousk, J., Wallander, H., & Casals, P. (2011). Microbial growth rate measurements reveal that land-use abandonment promotes a fungal dominance of SOM decomposition in grazed Mediterranean ecosystems. *Biology and Fertility of Soils*, *47*(2), 129–138. <https://doi.org/10.1007/s00374-010-0510-8>
- Lorimer, G. H., & Pierce, J. (1989). Carbonyl sulfide—An alternate substrate for but not an activator of ribulose-1,5-bisphosphate carboxylase. *Journal of Biological Chemistry*, *264*(5), 2764–2772.
- Marschner, B., Brodowski, S., Dreves, A., Gleixner, G., Gude, A., Grootes, P. M., et al. (2008). How relevant is recalcitrance for the stabilization of organic matter in soils? *Journal of Plant Nutrition and Soil Science*, *171*(1), 91–110. <https://doi.org/10.1002/jpln.200700049>
- Masaki, Y., Ozawa, R., Kageyama, K., & Katayama, Y. (2016). Degradation and emission of carbonyl sulfide, an atmospheric trace gas, by fungi isolated from forest soil. *FEMS Microbiology Letters*, *363*(18), 7. <https://doi.org/10.1093/femsle/fnw197>
- Maseyk, K., Berry, J. A., Billesbach, D., Campbell, J. E., Torn, M. S., Zahniser, M., & Seibt, U. (2014). Sources and sinks of carbonyl sulfide in an agricultural field in the Southern Great Plains. *Proceedings of the National Academy of Sciences of the United States of America*, *111*(25), 9064–9069. <https://doi.org/10.1073/pnas.1319132111>
- McClelland, G. H., & Judd, C. M. (1993). Statistical difficulties of detecting interactions and moderator effects. *Psychological Bulletin*, *114*(2), 376–390. <https://doi.org/10.1037/0033-2909.114.2.376>
- Meredith, L., Boye, K., Youngerman, C., Whelan, M., Ogée, J., Sauze, J., & Wingate, L. (2018). Coupled biological and abiotic mechanisms driving carbonyl sulfide production in soils. *Soil Systems*, *2*(3), 37.
- Meredith, L. K., Ogée, J., Boye, K., Singer, E., Wingate, L., Von Sperber, C., et al. (2019). Soil exchange rates of COS and CO<sub>18</sub>O differ with the diversity of microbial communities and their carbonic anhydrase enzymes. *The ISME Journal*, *13*(2), 290–300. <https://doi.org/10.1038/s41396-018-0270-2>
- Mikutta, R., Kleber, M., Torn, M. S., & Jahn, R. (2006). Stabilization of soil organic matter: Association with minerals or chemical recalcitrance? *Biogeochemistry*, *77*(1), 25–56. <https://doi.org/10.1007/s10533-005-0712-6>
- Montzka, S. A., Calvert, P., Hall, B. D., Elkins, J. W., Conway, T. J., Tans, P. P., & Sweeney, C. (2007). On the global distribution, seasonality, and budget of atmospheric carbonyl sulfide (COS) and some similarities to CO<sub>2</sub>. *Journal of Geophysical Research-Atmospheres*, *112*(D9). <https://doi.org/10.1029/2006jd007665>
- Mu, Y. J., Geng, C. M., Wang, M. Z., Wu, H., Zhang, X. S., & Jiang, G. B. (2004). Photochemical production of carbonyl sulfide in precipitation. *Journal of Geophysical Research-Atmospheres*, *109*(D13). <https://doi.org/10.1029/2003jd004206>
- Noe, S. M., Kimmel, V., Hüve, K., Copolovici, L., Portillo-Estrada, M., Püttsepp, Ü., et al. (2011). Ecosystem-scale biosphere-atmosphere interactions of a hemiboreal mixed forest stand at Jarvelja, Estonia. *Forest Ecology and Management*, *262*(2), 71–81. <https://doi.org/10.1016/j.foreco.2010.09.013>
- Noe, S. M., Niinemets, Ü., Krasnova, A., Krasnov, D., Motallebi, A., Kängsepp, V., et al. (2015). SMEAR Estonia. *Perspectives of a large-scale forest ecosystem—Atmosphere research infrastructure*, *63*(1), 56. <https://doi.org/10.1515/fsmu-2015-0009>
- Ogawa, T., Kato, H., Higashide, M., Nishimiya, M., & Katayama, Y. (2016). Degradation of carbonyl sulfide by Actinomycetes and detection of clade D of beta-class carbonic anhydrase. *FEMS Microbiology Letters*, *363*(19), 9. <https://doi.org/10.1093/femsle/fnw223>
- Ogawa, T., Noguchi, K., Saito, M., Nagahata, Y., Kato, H., Ohtaki, A., et al. (2013). Carbonyl sulfide hydrolase from *Thiobacillus thioparus* strain TH1115 is one of the beta-carbonic anhydrase family enzymes. *Journal of the American Chemical Society*, *135*(10), 3818–3825. <https://doi.org/10.1021/ja307735e>
- Ogée, J., Sauze, J., Kesselmeier, J., Genty, B., Van Diest, H., Launois, T., & Wingate, L. (2015). A new mechanistic framework to predict OCS fluxes from soils. *Biogeosciences Discussions*, *12*(18), 15,687–15,736. <https://doi.org/10.5194/bgd-12-15687-2015>
- Ogée, J., Sauze, J., Kesselmeier, J., Genty, B., Van Diest, H., Launois, T., & Wingate, L. (2016). A new mechanistic framework to predict OCS fluxes from soils. *Biogeosciences*, *13*(8), 2221–2240. <https://doi.org/10.5194/bg-13-2221-2016>
- Perez-Priego, O., El-Madany, T. S., Migliavacca, M., Kowalski, A. S., Jung, M., Carrara, A., et al. (2017). Evaluation of eddy covariance latent heat fluxes with independent lysimeter and sapflow estimates in a Mediterranean savannah ecosystem. *Agricultural and Forest Meteorology*, *236*, 87–99. <https://doi.org/10.1016/j.agrformet.2017.01.009>
- Pilegaard, K., Ibrom, A., Courtney, M. S., Hummelshøj, P., & Jensen, N. O. (2011). Increasing net CO<sub>2</sub> uptake by a Danish beech forest during the period from 1996 to 2009. *Agricultural and Forest Meteorology*, *151*(7), 934–946. <https://doi.org/10.1016/j.agrformet.2011.02.013>
- R Core Team (2018). *R: A language and environment for statistical computing*, R Foundation for Statistical Computing (Version 3.5.0), (). Vienna: Austria. Retrieved from. <https://www.R-project.org/>
- Rayment, M. B., & Jarvis, P. G. (1997). An improved open chamber system for measuring soil CO<sub>2</sub> effluxes in the field. *Journal of Geophysical Research-Atmospheres*, *102*(D24), 28,779–28,784. <https://doi.org/10.1029/97jd01103>
- RStudio Team (2016). *RStudio: Integrated Development for R*. Boston, MA: RStudio Inc. Retrieved from. <http://www.rstudio.com/>
- Sandoval-Soto, L., Stanimirov, M., von Hobe, M., Schmitt, V., Valdes, J., Wild, A., & Kesselmeier, J. (2005). Global uptake of carbonyl sulfide (COS) by terrestrial vegetation: Estimates corrected by deposition velocities normalized to the uptake of carbon dioxide (CO<sub>2</sub>). *Biogeosciences*, *2*(2), 125–132.
- Sardans, J., & Penuelas, J. (2005). Drought decreases soil enzyme activity in a Mediterranean *Quercus ilex* L. forest. *Soil Biology & Biochemistry*, *37*(3), 455–461. <https://doi.org/10.1016/j.soilbio.2004.08.004>
- Sauze, J., Ogée, J., Maron, P. A., Crouzet, O., Nowak, V., Wohl, S., et al. (2017). The interaction of soil phototrophs and fungi with pH and their impact on soil CO<sub>2</sub>, (COO)-O-18 and OCS exchange. *Soil Biology & Biochemistry*, *115*, 371–382. <https://doi.org/10.1016/j.soilbio.2017.09.009>
- Seefeldt, L. C., Rasche, M. E., & Ensign, S. A. (1995). Carbonyl sulfide and carbon-dioxide as new substrates, and carbon-disulfide as a new inhibitor, of nitrogenase. *Biochemistry*, *34*(16), 5382–5389. <https://doi.org/10.1021/bi00016a009>
- Seibt, U., Kesselmeier, J., Sandoval-Soto, L., Kuhn, U., & Berry, J. A. (2010). A kinetic analysis of leaf uptake of COS and its relation to transpiration, photosynthesis and carbon isotope fractionation. *Biogeosciences*, *7*(1), 333–341.
- Seibt, U., Wingate, L., Lloyd, J., & Berry, J. A. (2006). Diurnally variable δ<sup>18</sup>O signatures of soil CO<sub>2</sub> fluxes indicate carbonic anhydrase activity in a forest soil. *Journal of Geophysical Research*, *111*(G4), n/a–n/a. <https://doi.org/10.1029/2006jg000177>
- Smeulders, M. J., Pol, A., Venselaar, H., Barends, T. R., Hermans, J., Jetten, M. S., & Op den Camp, H. J. (2013). Bacterial CS<sub>2</sub> hydrolases from *Acidithiobacillus thiooxidans* strains are homologous to the archaeal catenane CS<sub>2</sub> hydrolase. *Journal of Bacteriology*, *195*(18), 4046–4056. <https://doi.org/10.1128/JB.00627-13>
- Steinbacher, M., Bingemer, H., & Schmidt, U. (2004). Measurements of the exchange of carbonyl sulfide (OCS) and carbon disulfide (CS<sub>2</sub>) between soil and atmosphere in a spruce forest in central Germany. *Atmospheric Environment*, *38*(35), 6043–6052. <https://doi.org/10.1016/j.atmosenv.2004.06.022>

- Stimler, K., Montzka, S. A., Berry, J. A., Rudich, Y., & Yakir, D. (2010). Relationships between carbonyl sulfide (COS) and CO<sub>2</sub> during leaf gas exchange. *New Phytologist*, *186*(4), 869–878. <https://doi.org/10.1111/j.1469-8137.2010.03218.x>
- Sun, W., Maseyk, K., Lett, C., & Seibt, U. (2015). A soil diffusion-reaction model for surface COS flux: COSSM v1. *Geoscientific Model Development*, *8*(10), 3055–3070. <https://doi.org/10.5194/gmd-8-3055-2015>
- Sun, W., Maseyk, K., Lett, C., & Seibt, U. (2016). Litter dominates surface fluxes of carbonyl sulfide in a Californian oak woodland. *Journal of Geophysical Research: Biogeosciences*, *121*, 438–450. <https://doi.org/10.1002/2015jg003149>
- Van Diest, H., & Kesselmeier, J. (2008). Soil atmosphere exchange of carbonyl sulfide (COS) regulated by diffusivity depending on water-filled pore space. *Biogeosciences*, *5*(2), 475–483.
- von Hobe, M. (2003). Photochemical and physical modeling of carbonyl sulfide in the ocean. *Journal of Geophysical Research*, *108*(C7). <https://doi.org/10.1029/2000jc000712>
- Wang, C. K., Yang, J. Y., & Zhang, Q. Z. (2006). Soil respiration in six temperate forests in China. *Global Change Biology*, *12*(11), 2103–2114. <https://doi.org/10.1111/j.1365-2486.2006.01234.x>
- Wehr, R., Commane, R., Munger, J. W., McManus, J. B., Nelson, D. D., Zahniser, M. S., et al. (2017). Dynamics of canopy stomatal conductance, transpiration, and evaporation in a temperate deciduous forest, validated by carbonyl sulfide uptake. *Biogeosciences*, *14*(2), 389–401. <https://doi.org/10.5194/bg-14-389-2017>
- Weiner, T., Gross, A., Moreno, G., Migliavacca, M., Schrupf, M., Reichstein, M., et al. (2018). Following the turnover of soil bioavailable phosphate in Mediterranean savanna by oxygen stable isotopes. *Journal of Geophysical Research: Biogeosciences*, *0*(123). <https://doi.org/10.1029/2017JG004086>
- Whelan, M. E., Hilton, T. W., Berry, J. A., Berkelhammer, M., Desai, A. R., & Campbell, J. E. (2016). Carbonyl sulfide exchange in soils for better estimates of ecosystem carbon uptake. *Atmospheric Chemistry and Physics*, *16*(6), 3711–3726.
- Whelan, M. E., Lennartz, S. T., Gimeno, T. E., Wehr, R., Wohlfahrt, G., Wang, Y., et al. (2018). Reviews and syntheses: Carbonyl sulfide as a multi-scale tracer for carbon and water cycles. *Biogeosciences*, *15*(12), 3625–3657. <https://doi.org/10.5194/bg-15-3625-2018>
- Whelan, M. E., & Rhew, R. C. (2015). Carbonyl sulfide produced by abiotic thermal and photodegradation of soil organic matter from wheat field substrate. *Journal of Geophysical Research: Biogeosciences*, *120*, 54–62. <https://doi.org/10.1002/2014jg002661>
- Wingate, L., Seibt, U., Maseyk, K., OgÉE, J., Almeida, P., Yakir, D. A. N., et al. (2008). Evaporation and carbonic anhydrase activity recorded in oxygen isotope signatures of net CO<sub>2</sub> fluxes from a Mediterranean soil. *Global Change Biology*, *14*(9), 2178–2193. <https://doi.org/10.1111/j.1365-2486.2008.01635.x>
- Wohlfahrt, G., Brill, F., Hörtnagl, L., Xu, X., Bingemer, H., Hansel, A., & Loreto, F. (2012). Carbonyl sulfide (COS) as a tracer for canopy photosynthesis, transpiration and stomatal conductance: potential and limitations. *Plant, Cell & Environment*, *35*(4), 657–667. <https://doi.org/10.1111/j.1365-3040.2011.02451.x>
- Wu, J., Larsen, K. S., van der Linden, L., Beier, C., Pilegaard, K., & Ibrom, A. (2013). Synthesis on the carbon budget and cycling in a Danish, temperate deciduous forest. *Agricultural and Forest Meteorology*, *181*, 94–107. <https://doi.org/10.1016/j.agrformet.2013.07.012>
- Yanni, S. F., Suddick, E. C., & Six, J. (2015). Photodegradation effects on CO<sub>2</sub> emissions from litter and SOM and photo-facilitation of microbial decomposition in a California grassland. *Soil Biology & Biochemistry*, *91*, 40–49. <https://doi.org/10.1016/j.soilbio.2015.08.021>
- Yi, Z. G., Wang, X. M., Sheng, G. Y., Zhang, D. Q., Zhou, G. Y., & Fu, J. M. (2007). Soil uptake of carbonyl sulfide in subtropical forests with different successional stages in south China. *Journal of Geophysical Research-Atmospheres*, *112*(D8), 11. <https://doi.org/10.1029/2006jd008048>
- Zeileis, A. (2004). Econometric computing with HC and HAC covariance matrix estimators. *Journal of Statistical Software*. doi:10.18637/jss.v011.i10
- Zepp, R. G., & Andreae, M. O. (1994). Factors affecting the photochemical production of carbonyl sulfide in seawater. *Geophysical Research Letters*, *21*(25), 2813–2816. <https://doi.org/10.1029/94gl03083>
- Zhang, L., Hu, Z., Fan, J., Zhou, D., & Tang, F. (2014). A meta-analysis of the canopy light extinction coefficient in terrestrial ecosystems. *Frontiers of Earth Science*, *8*(4), 599–609. <https://doi.org/10.1007/s11707-014-0446-7>
- Zuur, A. F., Ieno, E. N., & Elphick, C. S. (2010). A protocol for data exploration to avoid common statistical problems. *Methods in Ecology and Evolution*, *1*(1), 3–14. <https://doi.org/10.1111/j.2041-210X.2009.00001.x>